Stabilizing the hexagonal diamond metastable phase in silicon nanowires

R Béjaud, O. Hardouin Duparc

Contents lists available at ScienceDirect

Computational Materials Science

journal homepage: http://ees.elsevier.com

Stabilizing the hexagonal diamond metastable phase in silicon nanowires

R. Béjaud, O. Hardouin Duparc *

LSI, Laboratoire des Solides Irradiés, CEA-DRF-IRAMIS, CNRS, École Polytechnique, Institut Polytechnique de Paris, Palaiseau, France

ARTICLE INFO

Keywords
Nanowires
Silicon
Germanium
Hexagonal diamond
Cubic diamond
Ab initio calculations
Chemical potential

ABSTRACT

At the nanoscale, the proportion of atoms at the surface of solids becomes significant, which may change the equilibrium of atomic edifices. In the case of silicon, experimental observations have evidenced indeed the presence of the hexagonal diamond (HD) metastable structure in as-grown nanowires of a few nm in diameter, as if that phase could become the stable one in such small objects. We present *ab initio* calculations that demonstrate the existence of stable domain for the HD structure in silicon nanowires. Surfaces of HD Si are first studied without and with hydrogen, including possible relaxations, and compared to CD Si surfaces, with a globally favourable energy ratio for HD surfaces. The energies of several plausible HD and CD Si NWs of different thicknesses are then calculated and compared to estimate their relative phase stabilities, again in favour of HD NWs, without and with hydrogen at surfaces. Analytically extrapolating the *ab initio* results as functions of bulk, surface and edge energy contributions, the main result is that HD Si NWs are intrinsically stable with respect to CD Si NWs for effective diameters up to only about 15 nm, for pure Si NWs as well as for surface hydrogenated NWs. Thicker HD NWs can thus only be metastable. This may explain why Si HD NWs are so difficult to grow. The diameter size limit for germanium, silicon's big brother, is three times smaller, making HD Ge NWs much less likely, in agreement with recent experimental attempts to grow Ge NWs.

1. Introduction

Although the hexagonal diamond (HD) structure can be seen as being to the cubic diamond (CD) structure what the hexagonal close packed structure is to the cubic close packed structure, it has never been observed at the bulk level neither in carbon nor silicon or germanium.[1] For carbon, the HD structure is known as the lonsdaleite structure but it turned out that what was thought as being observed lonsdaleite actually is faulted and twinned cubic diamond [1]. The stable phase of bulk silicon is CD and HD bulk silicon has never been observed per se, only locally in high temperature indentation of CD, see Eremenko and Nikitenko [2], thanks to a mechanism occuring at twin-twin intersections during deformation twinning [3]. Nanophases, or structures for nanocrystals, may show different characteristics because of the importance of the surfaces in nanoparticles. It will naturally depend on the sizes and shapes of the nanoparticles. One must be very careful, though, since some silicon nanowires thought to be HD nanowires turned out to be nanotwinned CD nanowires [4].

Band structure calculations have shown that 2H nanowires of silicon with diameters slightly larger than 1 nm exhibit a direct bandgap [5–7] which can be very useful for, e.g., photovoltaic applications. Silicon nanowires are usually grown using the vapour-liquid-solid (VLS) process [8]. The latter is based on the precipitation of silicon atoms from a liquid metallic particle made of a low-temperature eutectic between silicon and a metal,[2] which acts as a catalyst for the growth: the silicon atoms are usually brought by chemical vapour deposition (CVD) with a silicon hydride (silane SiH_4, disilane Si_2H_6, etc.) as precursor gas; the gas molecules crack upon contact with the catalyst and deliver silicon in it; after saturation is reached, determined by the temperature of the particle and the liquidus line of the Si-metal system, silicon atoms precipitate out of the droplet onto a substrate in the form of a nanowire. The synthesis of 2H SiNWs using this method has probably been achieved in 2007 [9,10] but it was observed with absolute certainty only once, in 2017 [11]. In this latter case, tin was used as catalyst[3] and the deposition method benefitted from the help of a radio-frequency silane-hydrogen plasma (the method is called plasma-enhanced CVD, PECVD). Such a plasma contains SiH_4 silane molecules as well as SiH_3 and H radicals.

The question naturally arises as to whether the HD NW phase is stable or just metastable with respect to CD NWs. In this paper, we investigate what informations can be obtained from *ab initio* total energy minimization calculations. Given the importance of surfaces in nanowires, we first study 3C and 2H surfaces. We then study very thin nanowires and extrapolate our results to thicker nanowires with analytical formu-

* Corresponding author.
E-mail addresses: romuald.bejaud@polytechnique.edu (R. Béjaud); olivier.hardouinduparc@polytechnique.edu (O. Hardouin Duparc)

https://doi.org/10.1016/j.commatsci.2020.110180
Received 24 August 2020; Received in revised form 20 October 2020; Accepted 10 November 2020
Available online xxx
0927-0256/

lae incorporating the relative contributions of bulk, surfaces and edges in nanowires. We carried out these calculations for two extreme cases: pure silicon in an inert environment and silicon with hydrogen saturated surfaces. The rôle of the hydrogen chemical potential is considered and discussed, in relation with experimental conditions. The case of germanium is also considered in parallel.

2. Methods and systems studied

2.1. DFT calculations

We use density functional theory (DFT) based on the pseudopotential-plane-wave method according to the implementation provided by the Vienna *ab initio* simulation package (VASP) [12]. Our calculations will be mainly done using the local density approximation (LDA), with the projector augmented wave method (PAW) [13], with valence wave functions expanded over plane-wave basis sets with a cutoff energy of 450 eV for Si and 600 eV for Ge (i.e. ~33 and 40 Ry, respectively).

The k-space integrals over the three-dimensional Brillouin zones are calculated as discrete sums over special points of the Brillouin zone (BZ), generated by the Monkhorst-Pack (MP) method. The optimal geometry is obtained using the conjugate-gradient method to minimize the total energy of the system with respect to the atomic coordinates.

The basic lattice parameters and cohesive energies we obtained and shall use thereafter for surface and nanowire calculations are the following: $a_c = 5.406$ and 5.644 Å, $E_{\mathrm{coh.3C}} = -5.961$ and −5.173 eV/at for the Si and Ge 3C phase, respectively, calculated with a mesh of 8 × 4 × 4 MP grid points for the 3C phase corresponding to 50 **k** points in the reduced Brillouin zone, and $a = 3.806$ and 3.981 Å, $c/a = 1.652$ and 1.646, $E_{\mathrm{coh.2H}} = -5.951$ and −5.157 eV/at for the Si and Ge 2H phase, calculated with a 8 × 4 × 4 Γ centered grid points (for hexagonal lattices, energies converge significantly faster with a Γ centered mesh). The 3C phase is more stable than the 2H phase, with an $E_{\mathrm{coh.2H}} - E_{\mathrm{coh.3C}}$ difference, to be renamed infra as $\delta\mu$, equal to 10 meV/at and 16 meV/at for silicon and germanium, respectively. This agrees well with values previously obtained by a similar study, viz. 10.7 and 16 meV/at, respectively [14].

Both structures being tetragonal covalent locally similar up to third neighbours included, their so-called zero-point energies (ZPEs) can a priori be expected to be very similar with a subsequent difference negligible with respect to the electronic energy difference. We checked this point and found ZPE differences of 0.5 meV for Si and 0.3 meV for Ge.[4]

[1] Both structures are tetravalent and only differ beyond third neighbour distances. The 'close-packed-plane' stackings of the two structures, HD and CD, are …ABABAB…and …ABCABC…, respectively, usually labelled 2H versus 3C in the Ramsdell notation (2H is two-layer stacking, AB, hexagonal, 3C is three-layer stacking, ABC, cubic). As is well-known, neither HD nor CD are really close-packed structures at the atomic level, and the stacking sequences would be more faithfully described as …AaBbAaBbAaBb…and …AaBbCcAaBbCc…, respectively. Note that the silicon 2H structure is also sometimes labelled W or WZ, and called wurtzite since it corresponds to the beta-ZnS structure, notwithstanding the fact that the two atoms of the unit motif are chemically different in beta-ZnS, similar in 2H-Si. The silicon 3C structure is also sometimes labelled ZB, from the zinc-blende structure of alpha-ZnS. In older studies about different structures of silicon, silicon 3C and silicon 2H were labelled Si-I and Si-IV, respectively. In this paper we will use CD or 3C and HD or 2H.

[2] For instance, the Au-Si system melts at 363 °C at 18.6% at. Si, vs. 1064 °C and 1414 °C for pure gold and pure silicon respectively.

[3] Tin melts at 232 °C and the Si-Sn eutectic point is very close to pure Sn.

[4] Note that whereas the 2H and 3C structures have similar energies for essential, structural, reasons, the graphite and diamond structures just happen to accidentally have very similar energies for carbon [15,16].

Table 1
Description of the nanowires considered in this study. Sections can be rectangular (rec), hexagonal (hex), or octagonal (octa). Facets are portions of S_k surfaces and edges E_k are distinguished through E^i_{nm} symbols, see main text in Section 2.4.

Phase	Growth direction	Section	$\{S_k\}$	$\{E_k\}$
3C	⟨110⟩	hexa	({100},{111}S)	$\{E^1_{11}, E^1_{12}\}$
	⟨110⟩	hexa	({100},{111}G)	$\{E^1_{11}, E^1_{12}\}$
	⟨111⟩	hexa	({110})	$\{E^1_{11}\}$
	⟨111⟩	hexa	({112})	$\{E^1_{11}\}$
	⟨111⟩	hexa	({112})	$\{E^2_{11}\}$
	⟨211⟩	hexa	({111},{113})	$\{E^1_{11}, E^1_{12}\}$
2H	⟨0001⟩	rect	($\{1\bar{1}00\}$S, $\{11\bar{2}0\}$)	$\{E^1_{12}\}$
	⟨0001⟩	rect	($\{1\bar{1}00\}$S, $\{11\bar{2}0\}$)	$\{E^2_{12}\}$
	⟨0001⟩	rect	($\{1\bar{1}00\}$G, $\{11\bar{2}0\}$)	$\{E^1_{12}\}$
	⟨0001⟩	rect	($\{1\bar{1}00\}$G, $\{11\bar{2}0\}$)	$\{E^2_{12}\}$
	⟨0001⟩	hexa	$\{1\bar{1}00\}$S	$\{E^1_{11}\}$
	⟨0001⟩	hexa	$\{1\bar{1}00\}$G	$\{E^1_{11}\}$
	⟨0001⟩	hexa	$\{11\bar{2}0\}$	$\{E^1_{11}\}$
	⟨0001⟩	hexa	$\{11\bar{2}0\}$	$\{E^2_{11}\}$
	⟨0001⟩	hexa	$\{11\bar{2}0\}$	$\{E^3_{11}\}$
	⟨0001⟩	octa	($\{1\bar{1}00\}$S, $\{11\bar{2}0\}$)	$\{E^1_{11}, E^1_{12}\}$

2.2. Free surfaces

We study surface structures and energies with slab models periodically arranged along the normal direction of the surfaces. The slabs are separated by a layer of vacuum sufficiently large to limit the periodic interactions between atoms belonging to two different surfaces. We kept this vacuum layer thickness constant and equal to 10 Å. This value has been chosen after convergence tests performed for differents surfaces. With such slab models, the (excess) energy of an S_k surface can be extracted from the total energy of a slab containing n silicon (germanium) atoms in a relaxed configuration via:

$$\gamma_{S_k} \cdot S_k = E_{tot}(n, S_k) - n \cdot E_{\mathrm{coh}} \tag{1}$$

S_k in the left-hand side product in Eq. (1), corresponds to the total S_k surface area contained in the slab box (thus with a factor 2 with respect to the product of the lateral dimensions of the box). γ_{S_k} is the usual so-called surface energy for an S_k surface. It is normally given in J/m^2 (SI units) but can also be given in eV/Å^2. The number of atom layers between the two surfaces is varied until convergence. This number is typically of the order of twenty or more. E_{coh} is the cohesive energy of a silicon (germanium) atom in a perfect crystal. This energy can also be labelled μ (μ_{Si} or μ_{Ge}), the chemical potential of the material in its crystalline state, $\partial E^{\mathrm{cryst}}/\partial n$. For surface energies, the considered crystalline structure is 3C for surfaces of CD silicon, 2H for surfaces of HD silicon. For the sake of notation consistency, we will renote the corresponding cohesive energies $E_{\mathrm{coh.Si3C}}$ and $E_{\mathrm{coh.Si2H}}$ defined in the previous Section 2.1 as $\mu_{\mathrm{Si-3C}}$ and $\mu_{\mathrm{Si-2H}}$, respectively (idem for germanium, mutatis mutandis). Surfaces are labelled as S_k in a general way and, more precisely when necessary, as $S_{(111)\mathrm{S}}$, $S_{(111)\mathrm{G}}$, $S_{(100)2\times1}$, $S_{(0001)\mathrm{S}}$, etc., following the usual surface crystallographic usage for CD and HD surfaces. The S or G subscript specifies whether a surface is created from a

so-called shuffle or glide plane.[5] Such S and G planes are shown for the case of HD surfaces in Fig. 1.a for (1 $\bar{1}$ 0 0) planes. Possible surface reconstructions are indicated with the commonly used *nxm* notations [19]. Illustrations are given in Fig. 1.b. Because of the nanowires we are going to study, see Section 2.4, we first studied 3C (1 0 0), (1 1 0), (1 1 1), (1 1 2) and (1 1 3) surfaces (see Tables 2 and 3). For 2H nanowires, the experimentally observed growth direction being [0 0 0 1] , we studied surfaces that contain this direction, viz. $\{1\bar{1}00\}$ surfaces (corresponding to planes known as the prismatic planes) and $\{11\bar{2}0\}$ surfaces. Although we investigated many reconstruction possibilities, we did not include those which imply large area reconstructions such as the 7 × 7 of the (1 1 1) surface or the c(4 × 2) of the (1 1 0) surface because for NWs the surface dimensions perpendicular to the growth directions are small and large area reconstructions are not expected. We will come back to this point at the end of Section 3.3.

Let us note that for surface calculations, we also carried out for the sake of comparison some calculations made using the generalized gradient approximation (GGA), first considering the commonly used PBE functional [20] but also using modified functionals such as the AM05[6] and the PBEsol functionals [21,22]. The results we obtained are not significantly different, see Section 3.1.

2.3. Hydrogenated surfaces and hydrogen activity

As explained in the introduction, VLS Si (Ge) NWs grow in an environment rich in hydrogen because Si (Ge) atoms are brought under the form of SiH_4 (GeH_4) molecules leaving H radicals in the gaseous environment coexisting with other products under plasma conditions (SiH_3, H_2, H radicals, …). One thus expects NW facets to be H saturated. To start with unlimited surfaces, the energy of an H saturated S_k surface, γ_{HS_k}, can be written as:

$$\gamma_{HS_k} \cdot S_k = E_{tot}(n, n_H, HS_k) - n \cdot \mu - n_H \cdot \mu_H \quad (2)$$

μ corresponds to the chemical potential of Si (Ge) in the 3C or the 2H phase, as defined in the previous section. The number of Si (Ge) atoms is n and n_H is the number of H atoms.

μ_H cannot be so precisely defined because it corresponds to the hydrogen chemical potential in the complex environment gas phase: *i*) the temperature T of the gas phase is generally unknown and may be of a few hundreds of Celsius in NW growth experiments, based on the measured temperature of the substrate, the pressure can be very low, of the order of 1 Pa, yet with large variations between different authors,[7] *ii*) the partial pressures are not known because hydrogen exists in various molecular forms in a sometimes partly ionised gas in plasma conditions. In typical experimental conditions for silicon (and quite similarly for germanium, mutatis mutandis) the gas made of SiH_4 also contains radicals such as SiH_3, SiH_2, H, as well as H_2, and ions such as H^+ etc. The relative proportions of all these molecules cannot be measured precisely enough to propose a reliable equation for μ_H. The most reasonable way to deal with the problem is to write μ_H as

$$\mu_H = \mu_H/SiH_4 + \Delta\mu_H \quad (3)$$

where μ_H/SiH_4 is the cohesive energy for an hydrogen atom in a SiH_4 molecule vs the cohesive energy of a Si-3C crystal, SiH_4 being the dominant source species for Si NWs growth[8] [24–26]. $\Delta\mu_H$ is a value which cannot be known exactly and will thus have to be considered as a free variable: $\Delta\mu_H$ can be negative if the temperature is high and the pressure low[9] but can also be positive due to the presence of radicals (the cohesive energy of an H atom is much less, in absolute value, in SiH_3 than in the bond-saturated SiH_4 molecule).

Stated more precisely, μ_{H/SiH_4} is the hydrogen chemical potential value below which an SiH_4 molecule will decompose into four hydrogen atoms and a silicon atom going into an Si-3C bulk crystal, at null temperature and pressure. It is deduced from:

$$E_{coh.SiH_4} = \mu_{Si-3C} + 4 \cdot \mu_{H/SiH_4} \quad (4)$$

Within the same PAW-LDA scheme, we obtained $\mu_{H/SiH_4} = -3.3$ eV. Note that we do not explicitly introduce the hydrogen ZPE contribution because it is similar in an SiH_4 molecule and at a silicon surface so that it cancels out and does not affect Eq. (2) or the other equations.

Consideration of the S_k silicon surfaces themselves, rather than just silicon bulk, will lead to surface dependent formulae, with the introduction of S_k desorbing $\Delta\mu_H$ values, hereafter labelled $\Delta\mu_H^{Skdesorb}$: an HS_k surface will get free from its adsorbed hydrogen for μ_H values such that γ_{HS_k} is larger than γ_{S_k}, which, using Eqs. (2) and (3) correspond to $\Delta\mu_H < \Delta\mu_H^{Skdesorb}$ with $\Delta\mu_H^{Skdesorb}$ being equal to

$$\Delta\mu_H^{Skdesorb} = \frac{1}{n_H}[E_{tot}(n, n_H, HS_k) - n \cdot \mu - n_H \cdot \mu_{H/SiH_4} - \gamma_{S_k} \cdot S_k] \quad (5)$$

Let us rephrase for clarity: S_k is more stable than HS_k for $\mu_H < \mu_{H/SiH_4} + \Delta\mu_H^{Skdesorb}$. One can thus note that this immediately confirms and rationalizes a previous remark according to which "nanowire terminated by H atoms is stabilized for high μ_H whereas the pristine nanowire is favourable for low μ_H." [26].

In principle, for $\mu_H > \mu_{H/SiH_4}$, bulk silicon in presence of hydrogen decomposes so as to make SiH_4 molecules. Yet given the fact that the environment in NW growth conditions is not just made of free hydrogen, we will also consider positive $\Delta\mu_H$ values.

2.4. Nanowires

Bulk periodicity is applied along the nanowire growth direction while 10 Åvacuum spaces separate the nanowire surfaces (facets) along transversal directions. The linear (excess) energy of a nanowire N_k of periodic length l_k can be expressed in a similar way as for a surface, see Eq. (1):

$$\Omega_{N_k} \cdot l_k = E_{tot}(n, N_k) - n \cdot \mu_{Si-3C} \quad (6)$$

[5] The sets of shuffle and glide planes are so named for historical reasons coming from the study of plasticity mechanisms in CD structures. Indeed, the dislocations contained in the shuffle set were initially considered mobile with the diffusion of atoms, whereas those contained in the glide set were considered mobile by gliding [18].

[6] From a purely technical point of view, let us mention that the AM05 functional may cause the Davidson algorithm to diverge in some cases, in our case when the vacuum layer is larger than 7 Å. Here we thank the VASP team for this piece of information. Allowing VASP to use another algorithm fixes the divergence problem, just to confirm the energy values already obtained with the 7 Åvacuum layer.

[7] Tang et al. 2017 [11] indicate 400 °C at 1 Torr, i.e. ~133 Pa, Wu et al. 2004 [23] indicate 435 °C at 100 Torr, i.e. ~ 13 kPa. Ross, Tersoff and Reuter used 10^{-8}–10^{-5} Torr, 500–650 °C, with disilane, Phys. Rev. Lett. 95 (2005) 146104. We recall, for the sake of convenience: 1 Torr ~ 133 Pa, 1 Pa = 10^{-2} mbar, 1 atm ~ 1 bar ~ 10^5 Pa). Another parameter, besides the choice of a substrate and catalyst, is the duration of the experiment.

[8] Northrup and Akiyama et al. consider μ_{H/SiH_4} as a zero reference for μ_H. Their μ_H thus corresponds to our $\Delta\mu_H$. We prefer our formulation which recalls the conventional definition of μ_H.

[9] because of the leading $-k_BT \ln\left[k_BT(2\pi m k_BT/h^2)^{3/2}/p\right]$ term for the chemical potential in a one-element gas phase at pressure p. The usual k_B and h symbols are used for the Boltzmann and Planck constants, respectively, and m is the mass of the molecule in the gas. See for instance Kangawa et al., Surf. Sci. 493 (2001) 178. Note that the formula provided in Akiyama et al.'s articles [25,26] contains a typographical mistake.

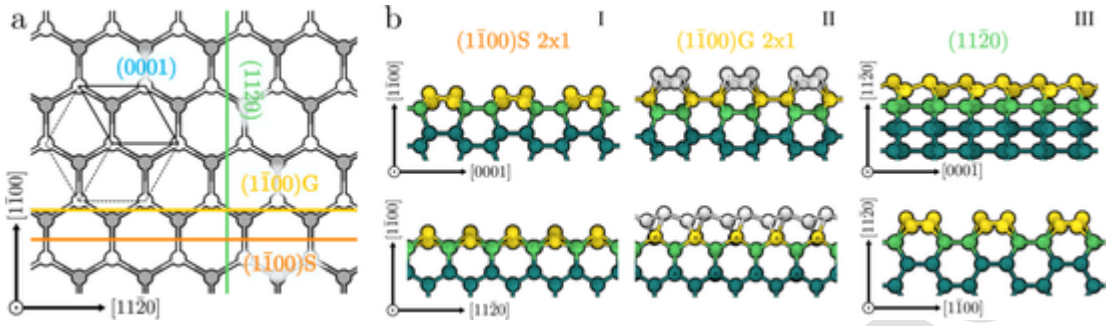

Fig. 1. Atomic illustration of the HD surfaces. (a) Top view of the (0001) surface showing in green the $(11\bar{2}0)$ planes and respectively in orange and yellow the "S" and "G" $(1\bar{1}00)$ planes. (b) Side view of the reconstructed HD surfaces. Atoms are colored according to their local atomic structures computed by analyzing the second nearest neighbours with the OVITO tools [17].

Table 2
3C and 2H free surface energies for silicon and germanium (relaxed). Values obtained in [30,31] for the (1 0 0), (1 1 0), (1 1 1) and (1 1 3) surfaces are given in parentheses. All other values are new.

Phase	Orientation	Reconstruction	Si			Ge		
			γ_S (J/m^2)		γ_S (eV/Å^2)	γ_S (J/m^2)		γ_S (eV/Å^2)
3C	(1 0 0)	none	2.274		0.142	1.553		0.097
	(1 0 0)	2 × 1	1.462	(1.45)	0.091	1.079	(1.05)	0.067
	(1 1 0)	none	1.700	(1.70)	0.106	1.212	(1.17)	0.076
	(1 1 1)	2 × 1	1.454	(1.45)	0.091	1.112	(1.05)	0.069
	(1 1 2)	2 × 1	1.565		0.098	1.143		0.071
	(1 1 3)	none	1.842	(1.85)	0.115	1.329	(1.29)	0.083
2H	(0 0 0 1)	none	1.581		0.099	1.182		0.074
	(1 $\bar{1}$ 0 0)G	tilted	1.683		0.105	1.197		0.075
	(1 $\bar{1}$ 0 0)G	2 × 1	1.553		0.097	1.112		0.069
	(1 $\bar{1}$ 0 0)S	2 × 1	1.310		0.082	0.964		0.060
	(1 1 $\bar{2}$ 0)	none	1.455		0.091	1.061		0.066

Note that for nanowires we use $\mu = \mu_{\mathrm{Si-3C}}$ (id. for Ge) whatever the CD or HD inner structure of the NW. This is because our goal for nanowires is to study the relative stability of HD versus CD NWs. Thick (nano) wires approach bulk conditions and CD wires are consequently more stable than HD wires. This condition is fulfilled by consistently using $\mu_{\mathrm{Si-3C}}$ in the previous expression for NW energies.

In the same way as for Eq. (2) in Section 2.3, we can define $\Omega_{\mathrm{H}N_k}$ for H saturated nanowires:

$$\Omega_{\mathrm{H}N_k} \cdot l_k = E_{tot}(n, n_{\mathrm{H}}, \mathrm{H}N_k) - n \cdot \mu_{\mathrm{Si-3C}} - n_{\mathrm{H}} \cdot \mu_{\mathrm{H}} \quad (7)$$

The nanowires we will study are described in Table 1. CD nanowires have been mainly observed with the $\langle 1\,1\,1 \rangle$ growth direction, but also with the $\langle 1\,1\,0 \rangle$ and $\langle 2\,1\,1 \rangle$ growth directions [27,23,28,29]. Experimental observations only report hexagonal cross-section shapes for these CD nanowires so that it is the shape considered in this study. One currently has no experimental information as for the possible cross-section shapes for HD NWs. The only certain 2H NWs observed so far were composed of an amorphous shell surrounding an ordered HD silicon phase core [11]. The growth direction is $[0\,0\,0\,1]$. We will explore three different types of cross-section shapes for 2H nanowires with this growth direction: rectangular, hexagonal and octagonal, with different facets and different edge types. As indicated in Section 2.2, some surfaces may exist as 'G-planes' or as 'S-planes'. For edges, globally noted as E_k, they result from the intersection of two surfaces which can be explicited as S_n and S_m with the additional fact that two surfaces can intersect in different ways leading to different local atomic structures with different associated energies, hence an additional l exponent in the more explicit E^l_{nm} notation for edges, as in Table 1 where all nanowire configurations tested in this study are reported. Since the lateral dimensions of the facets are small and all facets end up by edges with their neighbouring facets, NWs will be first built without imposing any surface pre-reconstruction, surface atoms will then be given small random displacements and relaxation is carried out. NW surface reconstructions will thus be obtained in a way fully compatible with the existence of edges.

We will define an effective diameter, D_{eff}, associated to each NW and based on the perimeter of its cross-section divided by π. This definition will allow to compare the energy stability of NWs with different cross-sections shapes, as a functions of their D_{eff} : $\Omega_{N_k}(D_{\mathrm{eff}})$ and $\Omega_{\mathrm{H}N_k}(D_{\mathrm{eff}})$, see Sections 3.3 and 3.4.

3. Results and discussions

3.1. Free surfaces

Free (pristine) surface energies are summarized in Table 2. They are given in the usual J/m^2 SI unit and in eV/Å^2 because later results, implying the hydrogen chemical potential, are always given in eV and Å(or nm, 10 Å = 1 nm). Let us first mention that besides the well-known CD surface reconstructions, we found the following reconstructions for HD surfaces: *i*) the (1$\bar{1}$00)S surface has a 2 × 1 reconstruction, see Fig. 1.b. This surface is composed of dimers where each atom (see yellow atoms in Fig. 1.b.I) has a dangling bond. After relaxation the dimers are tilted: one atom per dimer is slightly away from the surface while the second is closer. This happens in opposite directions for neighbouring dimers, resulting in a 2 × 1 reconstruction, *ii*) The

Table 3
3C and 2H hydrogenated surface energies for silicon and germanium computed for $\Delta\mu_H$ = -0.4, 0 and 0.4 eV. The critical $\Delta\mu_H^{Skdesorb}$ values that desorb hydrogen from S_k surfaces are also reported.

Phase	Orientation		γ_{HS_k} (eV/Å^2)			$\Delta\mu_H^{Skdesorb}$ (eV)
			$\Delta\mu_H$ = -0.4 eV	$\Delta\mu_H$ = 0 eV	$\Delta\mu_H$ = 0.4 eV	
Si(3C)	(1 0 0)		0.0705	0.0157	−0.0391	−1.354
	(1 0 0)	2 × 1	0.0409	0.0135	−0.0139	−1.135
	(1 1 0)		0.0415	0.0028	−0.0360	−1.063
	(1 1 1) S		0.0350	0.0033	−0.0283	−1.540
	(1 1 1) G		0.0976	0.0026	−0.0923	−2.785
	(1 1 2)		0.0654	0.0318	−0.0018	−0.786
	(1 1 3)		0.0535	0.0045	−0.0444	−0.977
Si(2H)	(0001)S		0.0302	0.0026	−0.0250	−1.391
	(0001)G		0.0851	0.0023	−0.0806	−2.768
	(1$\bar{1}$00)S		0.0378	l0.0043	−0.0291	−0.926
	(1$\bar{1}$00)G		0.0709	0.0040	−0.0630	−0.556
	(1$\bar{1}$00)G	2 × 1	0.0513	0.0179	−0.0156	−0.945
	(11$\bar{2}$0)		0.0428	0.0041	−0.0345	−0.897
Ge(3C)	(1 0 0)		0.0600	0.0100	−0.0403	−0.696
	(1 0 0)	2 × 1	0.0406	0.0155	−0.0095	−1.300
	(1 1 0)		0.0411	0.0056	−0.0299	−0.790
	(1 1 1) S		0.0332	0.0042	−0.0247	−0.894
	(1 1 1) G		0.0864	−0.0005	−0.0874	−2.391
	(1 1 2)		0.0604	0.0296	−0.0011	−0.542
	(1 1 3)		0.0529	0.0075	−0.0379	−0.782
Ge(2H)	(0001)S		0.0268	0.0015	−0.0237	−1.146
	(0001)G		0.0757	0.0000	−0.0757	−0.823
	(1$\bar{1}$00)S		0.0361	0.0054	−0.0252	−0.715
	(1$\bar{1}$00)G		0.0663	0.0050	−0.0563	−0.421
	(1$\bar{1}$00)G	2 × 1	0.0480	0.0173	−0.0133	−0.680
	(11$\bar{2}$0)G		0.0415	0.0061	−0.0293	−0.680

(1$\bar{1}$00)G surface is also composed of dimers but each atom originally has two dangling bonds. During relaxation, dimers rotate by an angle close to 45 ° that permits to form bonds with neighbour dimers. The 2 × 1 reconstruction is obtained when two neighbour dimers are rotated respectively by 45 ° and −45 ° angle, *iii*) For the (11$\bar{2}$0) surface, we only observe local relaxations of the surface atoms with slight shifts from their original positions (see yellow atoms in Fig. 1.b.III).

As said in Section 2.2, we also used different DFT schemes more sophisticated than DFT LDA. The obtained ratios between the surface energies are similar within less than 8% between LDA and PBE or AM05 or PBEsol, meaning for instance that $\gamma_{(11\bar{2}0)}/\gamma_{(1\bar{1}00)S}$ remains between 1.10 and 1.12. This means that LDA is accurate enough for this study.

The most important conclusion is that among the surfaces we studied, the 2H (HD) (1$\bar{1}$00) surface has the lowest energy, in its (1$\bar{1}$00)S 2 × 1 reconstructed form, followed by the 2H (11$\bar{2}$0) and the 3C (1 1 1) 2 × 1 reconstructed surfaces (one caveat is that large CD surface reconstructions have energies of the order of low energy HD surface, but these large surface reconstructions are not expected for small NWs).

Comparing Si and Ge, surface energies are smaller for Ge: germanium being less cohesive than silicon (by about 10%) with lattice parameters slightly larger (by about 5%), the Ge γ_{S_k} are consistently smaller than Si γ_{S_k} (by about 25%). We find that if the energy classification of surfaces is closely the same, energy differences between two surfaces are almost always lower between Ge surfaces than between Si surfaces.

This first set of calculations indicates that some 2H NWs described in Table 1 might have lower energies than the 3C NWs described in the same table because their 2H related surfaces are of lower energies than the corresponding 3C surfaces. It also indicates that this possible effect, if confirmed, will be less pronounced for Ge than for Si NWs.

3.2. H-terminated surfaces

The extreme opposite case to free surfaces is hydrogen saturated surfaces. Their energies γ_{HS_k} are obtained using Eq. (2) and the resulting values are plotted in Fig. 2.a while explicit numerical values are reported in Table 3 for three different $\Delta\mu_H$ values, $\Delta\mu_H$ = −0.4, 0, and 0.4 eV, for both Si and Ge (our seemingly arbitrary choice of −0.4 eV is justified infra). Each surface energy appears to be $\Delta\mu_H$ linearly dependent. This can actually be simply and directly demonstrated from Eqs. (2) and (3): expressing γ_{HS_k} as a function of μ_H, one gets

$$\gamma_{HS_k}(\mu_H) = \gamma_{HS_k}(\mu_H = \mu_{H/SiH_4}) - (n_H/S_k)\Delta\mu_H \quad (8)$$

The slope n_H/S_k corresponds to $n_{H/Si}/S_{k/Si}$, where $n_{H/Si}$ is the number of hydrogens per surface Si atom, which can be called H:Si ratio, and $S_{k/Si}$ is the surface area per Si atom for the S_k surface. Fig. 2.a shows that S-surfaces (green curves) are stable for large negative $\Delta\mu_H$ values whereas G-surfaces (pink and violet curves) have a lower energy for large positive $\Delta\mu_H$ values. This observation can easily be explained using the previous comments, as shown and numerically developed in the Appendix. Hence, considering all the studied surfaces, the (1 1 1) and (0 0 0 1) do happen to be the surfaces with the lowest energies in 'G' configurations for $\mu_H \gg \mu_{H/SiH_4}$ and in 'S' configurations for $\mu_H \ll \mu_H/SiH_4$. Considering only surfaces that contain the [0 0 0 1] or the [1 1 1] directions which are the most commonly observed NW growth directions, surfaces that turn out to have the lowest energies for a given μ_H are either (1$\bar{1}$00)S, (110) or (1$\bar{1}$00)G (see Fig. 2.b): the hydrogenated (1$\bar{1}$00)S surface is the most stable one for $\Delta\mu_H < -0.12$ eV, the

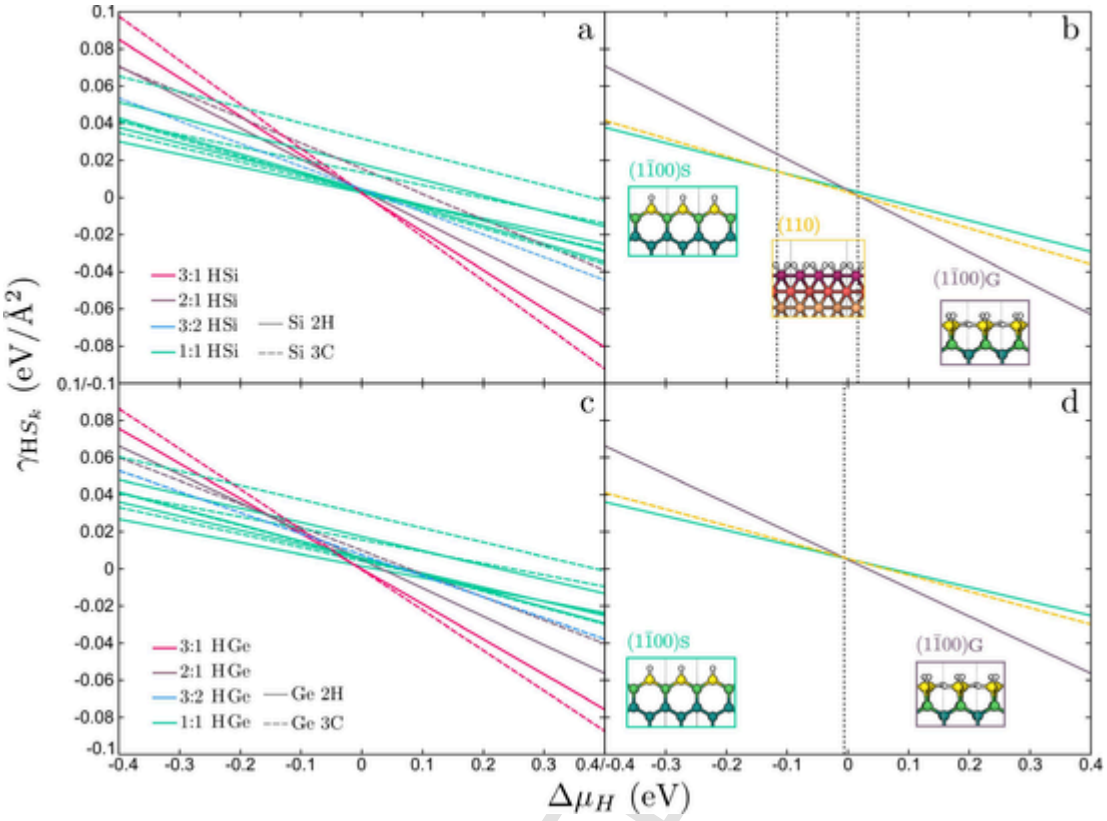

Fig. 2. H-terminated surface energies as functions of $\Delta\mu_H$ for Si: (a) and Ge: (c). With respect to figures (a) and (c), figures (b) and (d) correspond to surfaces that have the lowest energies for a given $\Delta\mu_H$, containing the [0001] or the [111] growth direction, for Si and, Ge respectively.

hydrogenated CD (110) surface is, albeit only very slightly, the preferred surface for intermediate μ_H values, -0.12 eV$<\Delta\mu_H<0.02$ eV) and the (1$\bar{1}$00)S surface is preferred for $\Delta\mu_H>0.2$ eV.

In Table 3, we also report the critical $\Delta\mu_H^{Skdesorb}$ values that desorb hydrogen from S_k surfaces, passing from hydrogenated surface HS_k to a free surface S_k, see Section 2.2 and Eq. (5). The 2H (1$\bar{1}$00)G has the highest $\mu_H^{Skdesorb}$ value, which means that it should be the first to be freed of its hydrogen on temperature raising or pressure decrease. According to Table 3, all the studied surfaces are expected to be H-saturated for $\Delta\mu_H$ values above -0.4 eV (within the $[-0.4, 0]$ eV range from a restrictive point of view, see the end of Section 2.3 where we explained why we also consider positive values of $\Delta\mu_H$).

Corresponding results for germanium are also given in Tables 2 and 3. As for the γ_{S_k}, the $\gamma_{HS_k}(\mu_H = \mu_{H/GeH_4})$ are significantly smaller than the $\gamma_{HS_k}(\mu_H = \mu_H/SiH_4)$. The predominant role of the slope coefficient n_{H/S_k} is similar (same H:Ge ratio which varies from 1 to 3 and comparable S_k's). The μ_H .14 eV large 3C domain numerically observed for HS_k silicon surfaces with only a very slight energy preference is not present for germanium, see Fig. 2.d.

3.3. Nanowires with free facets

Previous results seem to indicate that the HD phase could be stabilized in nanostructures thanks to the low energies of HD surfaces versus CD surfaces. This indication needs to be confirmed.

We carried out relaxation calculations on nanowires of different cross-section shapes according to what is observed experimentally, see Section 2.4 and Table 1. We did it for effective diameters D_{eff} (perimeter/π) varying from 10 to 55 Å. The energies are reported in Fig. 3.a. The most energetically favourable configurations within this diameter range correspond to HD nanowires with the [0001] growth direction. Three such types of NWs are particularly stable: the first two types are rectangular cross-section shaped with two $\{1\bar{1}00\}$S 2 × 1 and two $\{11\bar{2}0\}$S surface facets (full blue and purple diamond symbols in Fig. 3.a), with different kinds of edges (see for instance line 2H 1 vs line 2H 2 in Table 1), and the third type of NW has a hexagonal cross-section shape, with six $\{1\bar{1}00\}$S surfaces with 2 × 1 reconstruction and $\{E_{11}^1\}$ edges (full green circle symbols in Fig. 3.a). In details, the first two types appear to be very slightly more stable for small diameters, up to 42 Å, and the third type tends to become the most stable one beyond this diameter. NWs with CD structures (empty symbols in Fig. 3.a) have higher energies than most of the HD NWs.

Yet, if the HD phase gives the lowest Ω_{N_k} values for NWs in the diameter range shown in Fig. 3.a, one knows it cannot be the case for thick NWs, as explained in Section 2.4. The question is then to estimate the critical effective diameter value D_c below which some 2H NWs are more stable than 3C NWs. The largest NWs reported in Fig. 3.a contain about 600 silicon atoms and we obviously cannot expect to directly estimate D_c with currently available DFT simulations. It is actually more interesting to develop an analytical model fitted on DFT numerical values that will allow us to estimate D_c.

Eq. (6) can be tentatively decomposed as follows, for CD and HD NWs respectively:

$$\text{CD}: \quad \Omega_{N_k} \cdot l_k = \gamma_{N_k} \cdot S_{N_k} + \Gamma_{N_k} \cdot l_k \tag{9a}$$

$$\text{HD}: \quad \Omega_{N_k} \cdot l_k = \gamma_{N_k} \cdot S_{N_k} + \Gamma_{N_k} \cdot l_k + n \cdot \delta\mu \tag{9b}$$

where:

The nanowires N_k are described in Table 1.

$\gamma_{N_k} = (1/S_{N_k}) \sum_{k=1}^{N} (\gamma_{S_k} \cdot S_k)$ is the NW averaged surface energy per units area, S_{N_k} the whole surface area of the NW. The γ_{S_k} are the NW facet surface energies as calculated in Section 3.1.

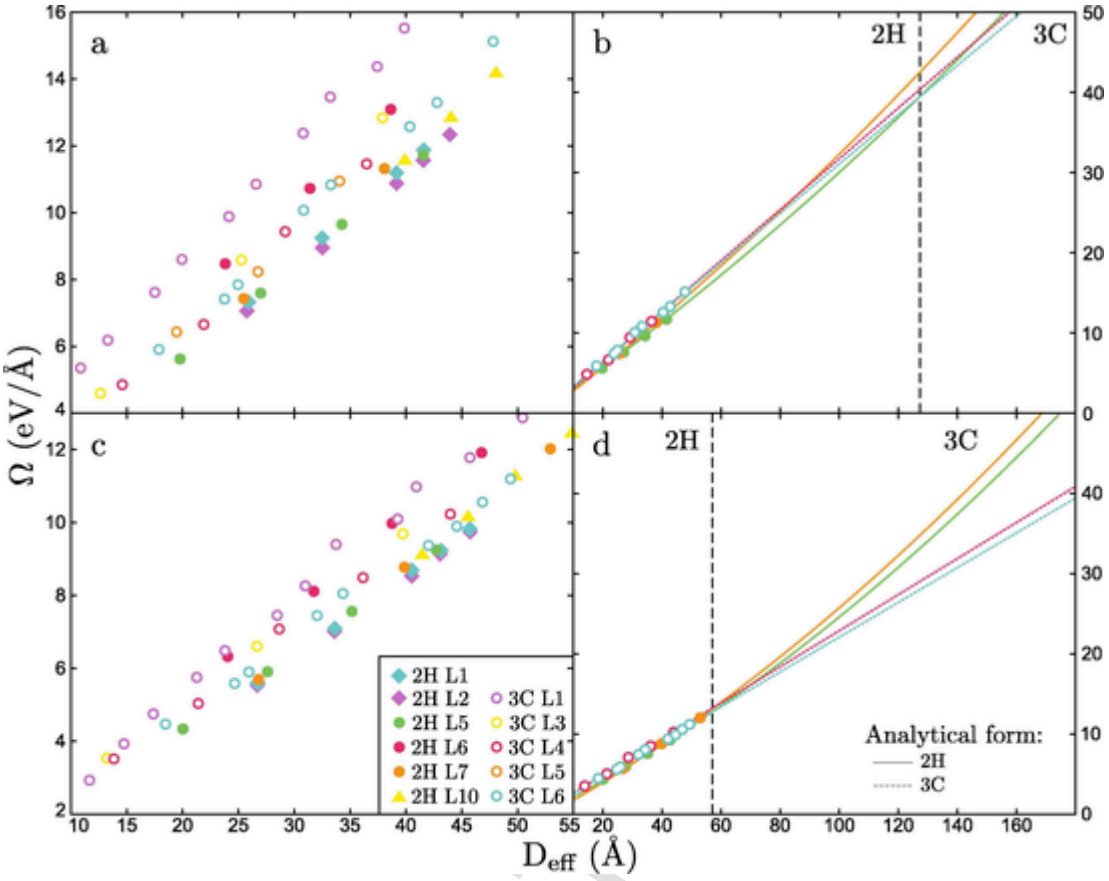

Fig. 3. Linear energy of Si NWs (a and b) and Ge NWs (c and d) with free surfaces, (a and c) calculated, and (b and d) extrapolated, see text. The plotted configurations are labelled according to their crystallographic structures and their position (line) in Table .1.

$\Gamma_{N_k} = \sum_{k=1}^{N} \Gamma_{E_k}$ is the energy formed by all of the E_k edges of the N_k NW. The Γ_{E_k} can be calculated by comparing, for example for the case of the E^1_{11} edge, the energy of a thick enough 2H [0 0 0 1] growth direction nanowire with six $\{1\,\bar{1}\,0\,0\}$S surfaces and six E^1_{11} edges to the corresponding following product $6\cdot\gamma_{(1\bar{1}00)S}\cdot S_{(1\bar{1}00)S}$ and divide the difference by 6. The quantitative value in this example is $E^1_{11} \sim 66.6$ meV/Åfor Si (57.6 meV/Åfor Ge).

The usual surface energies γ_{S_k}, as defined by Eq. (1) in Section 3.1 are referenced to the energies of their bulk counterparts. The same is true for the edge energies calculated as indicated just above. By contrast, the nanowire energies are always referenced to the 3C bulk energy because the goal is to study the stability of 2H NWs versus 3C NWs (see Eq. (6) in Section (2.4)). This explains the last term in Eq. (9b) (2H case): $\delta\mu$ is the cohesive energy difference between the HD and the CD phase, $\delta\mu = \mu_{Si-2H} - \mu_{Si-3C}$. It is multiplied by n, the number of Si atoms in the nanowire.

Eqs. (9a) and (9b) can be rewritten as functions of the NW diameter D_{eff} because $S_{N_k} = \pi\cdot D_{\text{eff}}\cdot l_k$and $n = (\pi D^2_{\text{eff}} l_k)/\,4V_{at}$ with V_{at} the atomic volume of Si atoms:

$$\text{CD}: \quad \Omega_{N_k}(D_{\text{eff}}) = \pi\cdot\gamma_{N_k}\cdot D_{\text{eff}} + \Gamma_{N_k} \tag{10a}$$

$$\text{HD}: \quad \Omega_{N_k}(D_{\text{eff}}) = \pi\cdot\gamma_{N_k}\cdot D_{\text{eff}} + \Gamma_{N_k} + \frac{\pi}{4V_{at}}\cdot\delta\mu\cdot D^2_{\text{eff}} \tag{10b}$$

Since $\delta\mu$ is positive, these two sets of equations clearly agree with the fact that HD nanowires must be energetically more costly than CD NWs for large values of D_{eff}. These equations will allow us to estimate the critical D_c between the two regimes.

For each N_k-type of nanowire, one can write the following analytical equation:

$$\Omega_{N_k}(D_{\text{eff}}) = a_N D^2_{\text{eff}} + b_{N_k} D_{\text{eff}} + c_{N_k} \tag{11}$$

The coefficient a_N is zero for 3C NWs and $\pi\cdot\delta\mu/\,4V_{at}$ for 2H NWs, the other coefficients b_{Nk} and c_{Nk} are determined by least-square fitting, linear (3C) or quadratic (2H), from DFT values obtained for D_{eff} values smaller than 50 Åshown in Fig. 3.a. D_c corresponds to the largest D_{eff} such that there exists a 2H-N_k curve which gives the lowest Ω_{N_k} value. As illustrated in Fig. 3.b, this critical diameter is found to occur for an approximate NW diameter of 130 Å. It results from the intersection between an HD N_k curve corresponding to nanowires with the [0 0 0 1] growth direction and $(1\,\bar{1}\,0\,0)$S 2×1 surfaces and the CD N_k curve corresponding to nanowires with the [2 1 1] growth direction and {1 1 1} and {1 1 3} surface facets.

For Ge nanowires, the three same stable configurations are found: the hexagonal cross-section NW with six $(1\,\bar{1}\,0\,0)$S 2×1 surface facets and the two rectangular cross-section NW with $(1\,\bar{1}\,0\,0)$S 2×1 and $(1\,1\,\bar{2}\,0)$ surfaces (see Fig. 3.c). A much lower critical diameter is obtained, $\sim$ 57 Å, corresponding again to the transition of an ($\langle 0\,0\,0\,1\rangle, \{1\,\bar{1}\,0\,0\}S2\times1$) HD nanowire to a ($\langle 2\,1\,1\rangle, \{1\,1\,1\}, \{1\,1\,3\}$) CD nanowire (see Fig. 3.d). The lower D_c value for germanium can be related the fact that the energy difference between HD and CD surfaces is less important for Ge than for Si (see Section 3.1).

Relatively thick NWs, with D_{eff} larger than 10 nm, have larger facets which can develop larger and more complex surface reconstructions with lower surface energies such as, for instance the CD (1 1 1)7×7 reconstruction, although edge effects could prevent the expected gain in energy except for D_{eff} much larger than 10 nm.

Favourable large complex surface reconstructions can also certainly occur for some HD NWs so that our estimation of a limit value of 15 nm for Si HD NWs remains a reasonable estimation.

3.4. Nanowires with H-terminated facets

As for surfaces, we also considered the extreme opposite case, viz NWs with surfaces fully saturated by hydrogen atoms. We carried out the same simulation procedures as in the previous subsection, with hydrogen atoms on top. Besides the role played by the hydrogen atoms in the DFT calculations, the final energy values Ω_{HN_k} also depend on the hydrogen chemical potential, see Eq. (7) (as well as (2) and (8)). The γ_{N_k} and Γ_{N_k} are accordingly replaced by γ_{HN_k} and Γ_{HN_k}. As in the previous subSection 3.3, we make use of the NW effective diameter D_{eff}:

$$\text{CD}: \quad \Omega_{HN_k} = \pi \cdot \gamma_{HN_k} \cdot D_{\text{eff}} + \Gamma_{HN_k} \tag{12a}$$

$$\text{HD}: \quad \Omega_{HN_k} = \pi \cdot \gamma_{HN_k} \cdot D_{\text{eff}} + \Gamma_{HN_k} \tag{12b}$$

$$+\frac{\pi}{4V_{at}} \cdot \delta\mu \cdot D_{\text{eff}}^2 \tag{12c}$$

The critical phase stability separating diameter D_c defined in subSection 3.3 now depends on μ_H (or $\Delta\mu_H$). We thus draw a 3C/2H static phase diagram for hydrogenated NWs as function of $\Delta\mu_H$ in abcissa and D_{eff} in ordinate. We actually distinguish between the different types of 3C or 2H NWs given in Table 1.

Fig. 4.a is a (non-Gibbsian) phase diagram which indicates the most stable NW configuration for a given (μ_H, D_{eff}) couple (it does not give relative frequencies between different competitive configurations). Six domains, among which four main ones, are found for Si NWs (left part of Fig. 4.a): three domains correspond to CD structures and three others to HD structures, only one of these last three corresponding to a significant domains. The three CD structures correspond to experimentally frequently observed ones [27,23,28,29]. They are here found to be the most stable ones for the following μ_H and D_{eff} ranges: ($\langle 111\rangle, \{110\}$) NWs (yellow domain) are energetically stable for low μ_H values and large enough D_{eff} values, ($\langle 110\rangle, \{001\}, \{111\}$G) NWs (purple domain) are energetically stable for large μ_H values, independently of D_{eff}, and there is also an intermediate regime where ($\langle 211\rangle, \{111\}, \{113\}$) NWs (blue domain) are energetically stable. Wu et al. [23] actually found a correlation between the diameters of the observed Si NWs and their growth directions, $\langle 111\rangle$ grown NWs being mainly observed for thick NWs (between 200 and 300 Å).[10] We additionally found a large low NW diameter and low μ_H domain where HD nanowires are stable. It actually consists of three HD NW domains: two very small and rather anecdotal domains (see the orange and red domains in Fig. 4.a corresponding to hexagonal cross-section NWs with respectively $\{11\bar{2}0\}$ and $\{1\bar{1}00\}$G surfaces) and one large green domain corresponding to hexagonal cross-section NWs with $\{1\bar{1}00\}$S surfaces.

In the same way as for non-hydrogenated nanowires, HD NWs are energetically stable when the NW diameter is small, <100 Å, for negative $\Delta\mu_H$ values, i.e. not too many radicals.

For Ge NWs, only three NW configurations are stable, see Fig. 4.b. The ($\langle 111\rangle, \{110\}$) NW configuration is not stabilized in Ge (this agrees with the fact that hydrogenated (110) surfaces are never the stable ones in Ge, see Section 3.2). The ($\langle 110\rangle, \{001\}, \{111\}$G) and ($\langle 211\rangle, \{111\}, \{113\}$) configurations are found to be energetically stable for CD NWs. For HD NWs, the ($\langle 0001\rangle, \{1\bar{1}00\}$S) configuration is still a stable one but the (μ_H, D_{eff}) domain in which this configuration is stabilised has been significantly reduced to small NWs diameters when compared to Si.

4. Summary and conclusions

It is a priori obvious that the stability of thin nanowires will be at least partly dictated by the stability of their surfaces. Yet accurate DFT calculations are necessary to be quantitatively more precise. One certainty from the stability point of view is that thick Si NWs must be 3C because $\mu_{\text{Si-3C}} < \mu_{\text{Si-2H}}$. As for surfaces possibly relevant for Si NWs, calculations made in this study show that the 2H surfaces are energetically lower than the 3C surfaces, substantially so for the $\{1\bar{1}00\}$S 2×1 surface (10% lower with respect to the (1 1 1) surface), see Table 2. So it may be expected that thin 2H NWs might be more stable than thin 3C NWs, see Section 3.1. Yet facets of thin NWs are clearly not comparable to infinite surfaces: besides forbidden large area reconstructions, facets additionally make edges with their contiguous facets in the direction where they are finite. Global and accurate calculations on NWs are therefore necessary to reappraise, and certify and quantify the relative stability issue. For pure NWs (or NWs in inert environment), several 2H [0001] NW configurations are found to be more stable than 3C NWs for small diameters between 10 and 50 Å, see Fig. 3.a. It proves necessary to extrapolate the DFT data with analytical formulae in order to estimate the critical effective diameter value D_c below which some 2H NWs are more stable than 3C NWs. We find $D_c \sim 130$ Å(13 nm) for silicon, and $D_c \sim 6$ nm for germanium.

Experimentalists, in order to grow Si or Ge NWs, need to use a metal catalyst, silver, gold or tin, deposited on an amorphous or crystalline silicon or silicon oxide substrate where it normally forms nanodropplets of various sizes, with vapour phases that contain mainly silane (SiH_4) molecules but also H_2, SiH_3 and other radicals in plasma conditions, at various temperatures and partial pressures during several minutes. DFT calculations cannot yet reproduce all this environmental complexity and kinetic conditions.[11] DFT calculations, however, allow to consider H covered surfaces. Still, they only provide $E_{tot}(n, n_H, HS_k)$ and $E_{tot}(n, n_H, HN_k)$ in Eqs. (2) and (7) respectively while γ_{HS_k} and Ω_{HN_k} given by these equations imply the use of the so-called chemical potential of hydrogen μ_H which is environment dependent and more difficult to define than the chemical potential of solid silicon μ which is simply a crystalline cohesive energy, viz. $\mu_{\text{Si-3C}}$ or $\mu_{\text{Si-2H}}$ in Eq. (2) and $\mu_{\text{Si-3C}}$ in Eq. (7). The chemical potential of hydrogen μ_H strongly depends on the milieu (environment) and the problem at hand, iron corrosion or silicon surface hydrogenation for instance. Albeit difficult to correlate to experimental conditions whatever the case, μ_H simply appears as a parameter in the energy Eqs. (2) and (7). Since we examine a physics involving silane molecules to grow silicon nanowires (or germane molecules to grow germanium nanowires), μ_H is best defined with respect to μ_{H/SiH_4} as in Eq. (4) (or with respect to μ_{H/GeH_4} in the germanium case). Our figures are drawn for μ_H values larger than $\mu_{H/SiH_4} - 0.4$ eV only so as to consider fully hydrogenated surfaces by contrast with the free surfaces we considered as a first case. The two independent parameters D_{eff} and μ_H led us to draw two-dimensional phase diagrams as in Fig. 4.a for Si NWs and Fig. 4.b for Ge NWs. Besides domains corresponding to effectively observed 3C Si NWs, a non negligible domain exists for 2H NWs, for negative $\Delta\mu_H$ and with D_{eff} which can probably reach ~ 150 Å(15 nm) for silicon, extrapolating Fig. 4.a leftwards for $\Delta\mu_H$ down to -0.92 eV which is the $\mu_H^{Skdesorb}$ desorbing value for the $\{1\bar{1}00\}$S surfaces of the relevant 2H NW, see

[10] Comparaison cannot be drawn further, however. Wu et alii [23] used gold droplets as catalysts deposited on oxydized silicon put in a quartz reactor, preheated their reactor at 435 °C, used SiH_4 and H_2 with a growth pressure maintained at 100 Torr (~13 kPa) during 30 min, see their article for details.

[11] This is a euphemism, of course. Analytical approaches are reviewed in [32]. Atomistic molecular dynamics simulations using semi-empirical potentials have been carried out in [33–35] and the phase-field method has been used in [36,37]. It is not the purpose of this contribution to review these complementary approaches.

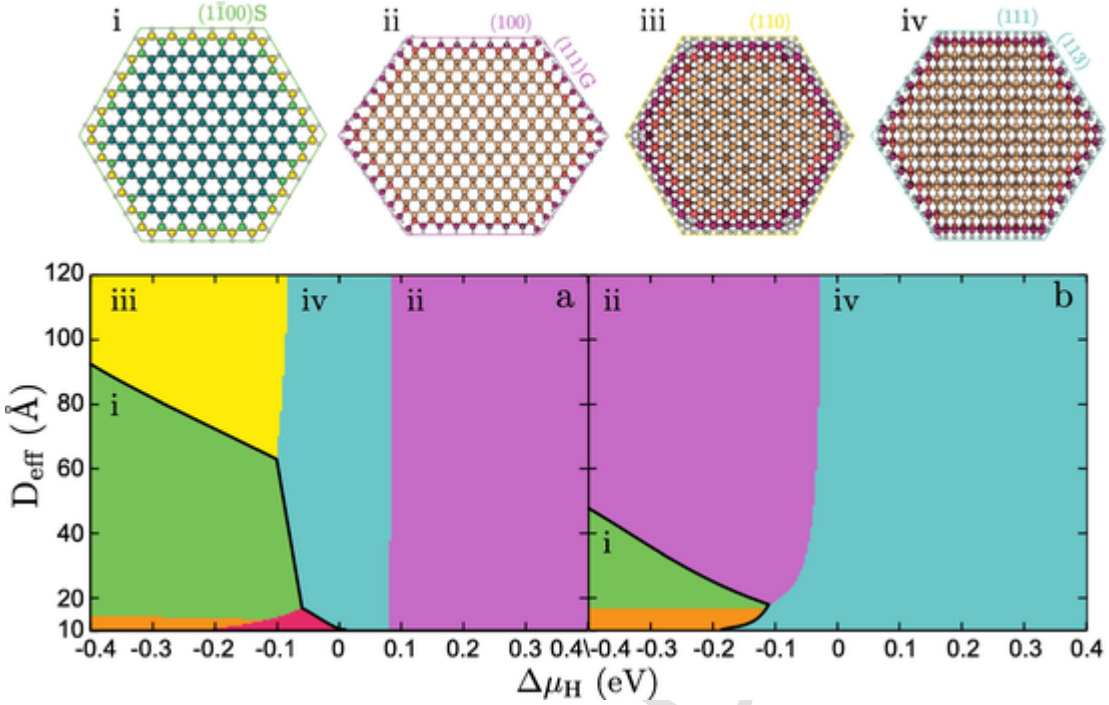

Fig. 4. $\Delta\mu_H$-D_{eff} diagrams showing the stable energy domains of HD and CD H-terminated nanowires for silicon on the left, (a), and for germanium on the right, (b). The four main stable domains are labelled i, ii, iii and iv and are further described in the text as ($\langle 0001\rangle$, $\{1\bar{1}00\}$S), ($\langle 110\rangle$, $\{001\}$, $\{111\}$G), ($\langle 111\rangle$, $\{110\}$) and ($\langle 211\rangle$, $\{111\}$, $\{113\}$), respectively. Above are atomic views of the cross-sections of these configurations. Atoms are colored according to their local atomic structures (see Fig. 1).

Table 3. This is consistently close to the value obtained when considering hydrogen free NWs only.

Germanium is clearly much less prone to stabilize HD NWs than silicon. This might sound surprising because germanium is often considered as an alter ego of silicon, simply bigger in size. It may, however, at least qualitatively be explained by the fact that germanium being less cohesive than silicon, effects observed in silicon will be less pronounced in germanium. Quantitatively, the change can only be obtained through first principle calculations as done in this work. It is in agreement with the fact that experimentalists have not yet been able to grow Ge HD NWs via the VLS route.

These results mean that experimentally obtained strain free 2H Si NWs with diameters above two nanometers can only be metastable. They also emphasize the rôle of the metal catalysts and all other experimental conditions which are necessary to make these 2H NWs especially if one wants much thicker hexagonal NWs in the future.

CRediT authorship contribution statement

R. Béjaud: Conceptualization, Methodology, Software, Validation, Formal analysis, Investigation, Data curation, Writing - original draft, Writing - review & editing, Visualization. **O. Hardouin Duparc:** Conceptualization, Validation, Resources, Writing - original draft, Writing - review & editing, Supervision, Project administration, Funding acquisition.

Declaration of Competing Interest

The authors declare that they have no known competing financial interests or personal relationships that could have appeared to influence the work reported in this paper.

Acknowledgements

This work was supported by the French National Research Agency (ANR) through the project HexaNW (reference ANR-17-CE09-0011). We thank our colleagues in this project for valuable discussions. Computations have been performed on supercomputer facilities using HPC resources from GENCI - CINES/IDRIS (Grant 2018-2019 – [A0050902210]) and using computer time granted by École Polytechnique through the LLR-LSI project.

Appendix A. Simple demonstration of the importance of the $-(n_H/S_k)\Delta\mu_H$ term in $\gamma_{HS_k}(\mu_H)$, Eq. (8)

Before reconstruction, S-surface atoms have only one dangling bond whereas G-surface atoms have two dangling bonds, as for $S_{(1\bar{1}00)G}$ (see Fig. 1.a), or even three, as for $S_{(111)G}$. Hence, because of the H:Si ratio n_H, the negative slope $-n_H/S_k$ in Eq. (8) is twice larger for (0 0 0 1) G versus (0 0 0 1) S, three times larger for (1 1 1) G than for (1 1 1) S. Numerically comparing n_H/S_k values pertaining to different surfaces, the largest and lowest values turn out to be very different: 0.237 Å^{-2} and 0.034 Å^{-2}, for the H(1 1 1) G and H(1 0 0)2 × 1 surfaces, respectively (the corresponding area $S_{k/Si}$ per surface Si atom are $a_c^2\sqrt{3}/4$ and a_c^2, and we use the a_c PAW-LDA silicon value found in Section 2.1, namely 5.406 Å). Since the DFT calculated $\gamma_{HS_k}(\mu_H = \mu_{H/SiH_4})$ values are in a relatively close range, between 0 and 0.032 eV/Å^2, the $-(n_H/S_k)\Delta\mu_H$ term rapidly makes the predominant differences between the surface energies γ_{HS_k} in Eq. (8), as can be seen in Fig. 2.a. Q.E.D.

References

[1] P. Németh, L.A.J. Garvie, T. Aoki, N. Dubrovinskaia, L. Dubrovinsky, P.R. Buseck, Lonsdaleite is faulted and twinned cubic diamond and does not exist as a discrete material, Nat. Commun. 5 (2014) 5447.
[2] V.G. Eremenko, V.I. Nikitenko, Electron microscope investigation of the microplastic deformation mechanisms of silicon by indentation, Physica Status Solidi (a) 14 (1972) 317.
[3] P. Müllner, P. Pirouz, A disclination model for the twin-twin intersection and the formation of diamond-hexagonal silicon and germanium, Mater. Sci. Eng.: A 233 (1997) 139.
[4] C. Cayron, M. Den Hertog, L. Latu-Romain, C. Mouchet, C. Secouard, J.-L. Rouvière, E. Rouvière, J.-P. Simonato, Odd electron diffraction patterns in silicon

nanowires and silicon thin films explained by microtwins and nanotwins, J. Appl. Crystallogr. 42 (2009) 242.
[5] X. Zhao, C.M. Wei, L. Yang, M.Y. Chou, Quantum confinement and electronic properties of silicon nanowires, Phys. Rev. Lett. 92 (2004) 236805.
[6] M. Amato, T. Kaewmaraya, A. Zobelli, P. Maurizia, Crystal phase effects in si nanowire polytypes and their homojunctions, Nano Lett. 16 (2016) 5694.
[7] S. Pandolfi, C. Renero-Lecuna, Y. Le Godec, B. Baptiste, N. Menguy, M. Lazzeri, C. Gervais, K. Spektor, W.A. Crichton, O. Kurakevych, Nature of hexagonal silicon forming via high-pressure synthesis: nanostructured hexagonal 4H polytype, Nano Lett. 18 (2018) 5989.
[8] R.S. Wagner, W.C. Ellis, Vapor-liquid-solid mechanism of single crystal growth, Appl. Phys. Lett. 4 (1964) 89.
[9] A. Fontcuberta i Morral, J. Arbiol, J. D. Prades, A. Cirera, J. R. Morante, Synthesis of silicon nanowires with wurtzite crystalline structure by using standard chemical vapor deposition, Adv. Mater. 19 (2007) 1347.
[10] J. Arbiol, B. Kalache, P. Roca i Cabarrocas, J. R. Morante, A. Fontcuberta i Morral. Influence of Cu as a catalyst on the properties of silicon nanowires synthesized by the vapour–solid–solid mechanism, Nanotechnology 18 (2007) 305606.
[11] J. Tang, J.-L. Maurice, F. Fossard, I. Florea, W. Chen, E. V. Johnson, M. Foldyna, L. Yu, P. Roca i Cabarrocas, Natural occurrence of the diamond hexagonal structure in silicon nanowires grown by a plasma-assisted vapour-liquid-solid method, Nanoscale 9 (2017) 8113.
[12] G. Kresse, J. Furthmüller, Efficiency of ab-initio total energy calculations for metals and semiconductors using a plane-wave basis set, Comput. Mater. Sci. 6 (1996) 15.
[13] P.E. Blöchl, Projector augmented-wave method, Phys. Rev. B 50 (1994) 17953.
[14] C. Raffy, J. Furthmüller, F. Bechstedt, Absolute surface energies of group-IV semiconductors: dependence on orientation and reconstruction, Phys. Rev. B 65 (2002) 115318.
[15] M.T. Yin, M.L. Cohen, Theory of static structural properties, crystal stability, and phase transformations: application to Si and Ge, Phys. Rev. B 26 (1982) 2199.
[16] M.T. Yin, M.L. Cohen, Structural theory of graphite and graphitic silicon, Phys. Rev. B 29 (1984) 6996.
[17] A. Stukowski, Visualization and analysis of atomistic simulation data with ovito-the open visualization tool, Model. Simul. Mater. Sci. Eng. 18 (2009) 015012.
[18] J.P. Hirth, J. Lothe, Theory of Dislocations, John Wiley & Sons Inc, 1982.
[19] E.A. Wood, Vocabulary of surface crystallography, J. Appl. Phys. 35 (1964) 1306.
[20] J.P. Perdew, K. Burke, M. Ernzerhof, Generalized gradient approximation made simple, Phys. Rev. Lett. 77 (1996) 3865.
[21] R. Armiento, A.E. Mattsson, Functional designed to include surface effects in self-consistent density functional theory, Phys. Rev. B 72 (2005) 085108.
[22] J.P. Perdew, A. Ruzsinszky, G.I. Csonka, O.A. Vydrov, G.E. Scuseria, L.A. Constantin, X. Zhou, K. Burke, Restoring the density-gradient expansion for exchange in solids and surfaces, Phys. Rev. Lett. 100 (2008) 136406.
[23] Y. Wu, Y. Cui, L. Huynh, C.J. Barrelet, D.C. Bell, C.M. Lieber, Controlled growth and structures of molecular-scale silicon nanowires, Nano Lett. 4 (2004) 433.
[24] J.E. Northrup, Structure of Si(100)H: dependence on the H chemical potential, Phys. Rev. B 44 (1991) 1419.
[25] T. Akiyama, K. Nakamura, T. Ito, Stacking sequence preference of pristine and hydrogen-terminated Si nanowires on Si(111) substrates, Phys. Rev. B 74 (2006) 033307.
[26] T. Akiyama, K. Nakamura, T. Ito, Structures and electronic properties of Si nanowires grown along the [110] direction: role of surface reconstruction, Surf. Sci. 602 (2008) 3033.
[27] D.D.D. Ma, C.S. Lee, F.C.K. Au, S.Y. Tong, S.T. Lee, Small-diameter silicon nanowire surfaces, Science 299 (2003) 1874.
[28] V. Schmidt, S. Senz, U. Gösele, Diameter-dependent growth direction of epitaxial silicon nanowires, Nano Lett. 5 (2005) 931.
[29] N. Shin, M.A. Filler, Controlling silicon nanowire growth direction via surface chemistry, Nano Lett. 12 (2012) 2865.
[30] A.A. Stekolnikov, J. Furthmüller, F. Bechstedt, Absolute surface energies of group-IV semiconductors: dependence on orientation and reconstruction, Phys. Rev. B 65 (2002) 115318.
[31] A.A. Stekolnikov, J. Furthmüller, F. Bechstedt, Adatoms, dimers, and interstitials on group-IV (113) surfaces: First-principles studies of energetical, structural, and electronic properties, Phys. Rev. B 67 (2003) 195332.
[32] V.G. Dubrovskii, Nucleation Theory and Growth of Nanostructures, Springer, Berlin, 2014.
[33] S. Ryu, W. Cai, Molecular dynamics simulations of gold-catalyzed growth of silicon bulk crystals and nanowires, J. Mater. Res. 26 (2011) 2199.
[34] H. Wang, L.A. Zepeda-Ruiz, G.H. Gilmer, M. Upmanyu, Structural theory of graphite and graphitic silicon, Nat. Commun. 4 (2013) 1956.
[35] T. Frolov, W.C. Carter, M. Asta, Capillary instability in nanowire geometries, Nano Lett. 14 (2014) 3577.
[36] Y. Wang, S. Ryu, P.C. McIntyre, W. Cai, A three-dimensional phase field model for nanowire growth by the vapor–liquid–solid mechanism, Modell. Simul. Mater. Sci. Eng. 22 (2014) 055005.
[37] N. Wang, M. Upmanyu, A. Karma, Phase-field model of vapor-liquid-solid nanowire growth, Phys. Rev. Mater. 2 (2018) 033402.